ELSEVIER

Polymer 41 (2000) 367–375

polymer

Rheology of strongly segregated poly(styrene–dimethylsiloxane) block copolymers

D. Rosati, B. Van Loon, P. Navard*

Ecole des Mines de Paris, Centre de Mise en Forme des Matériaux, UMR CNRS 7635, BP 207, F-06904 Sophia Antipolis, France

Received 15 April 1998; received in revised form 3 February 1999; accepted 4 February 1999

Abstract

Strongly segregated poly(styrene–dimethylsiloxane) di- and triblock copolymers were studied by dynamic rheological measurements at the extreme of the linear regime, below the order-to-disorder transition. The copolymers had lamellar and cylindrical microstructures. Applying the time–temperature superposition principle to the high-frequency range of the loss modulus gives a shift factor which enables G' and G'' master curves to be plotted at high reduced frequencies, where the effects of the microstructure and the large scale granular morphology are not important. Two critical frequencies can be determined, ω_c' where the shift factor determined from the loss modulus fail to superimpose the storage modulus, and $\omega_c'' \ll \omega_c'$ where the loss modulus curves do not superimpose. This is very clear for the diblock and the triblock with the lamellar microstructure. The departure from the time–temperature master curves is more pronounced when going from the cylindrical diblock to the lamellar diblock, and also to the lamellar triblock. This is explained by a connectivity term which expresses the difficulty of high connectivity structures (like lamellar arrangements or microdomains "anchored" by triblock molecules) to accommodate deformation without significant irreversible distortions (i.e. orientation).

Keywords: Block copolymer; Polystyrene; Polydimethylsiloxane

1. Introduction

Microphase-separated di- and triblock copolymers are known to form various distinct periodic microstructures (spheres, bicontinuous phases, cylinders or lamellae) as either the temperature is lowered or the molecular weight is increased [1,2]. Considering the microphases of highest symmetry (i.e. lamellar or cylindrical), spatial coherency of quenched and solvent-cast samples is low at intermediate length scales (~10 nm to 1 μm) because of topological defects [3–5]. Consequently, without the application of an orientational field, lamellar and cylindrical phase-separated block copolymers are isotropic at a global scale (~1 μm to 1 mm), exhibiting complex granular or "polycrystalline" morphologies.

The occurrence of a phase-separated morphology strongly affects the linear viscoelastic response of the system, especially at long time/low frequency [6]. Well above the order-to-disorder transition (often termed the ODT), the viscoelastic response is polymer-liquid like, with a well-defined, single relaxation-time terminal behaviour ($G' \propto \omega^2$ and $G'' \propto \omega$). On the contrary, far below the ODT, the response is "power-law like" ($G' \sim G'' \propto \omega^{0.3–0.7}$) over a wide range of frequencies, including the terminal-zone of the disordered sample. Near the transition, composition fluctuations influence the viscoelastic response in the terminal-zone. In the disordered state, deformation of the pre-transitional fluctuating structure is expected to induce additional elastic stress and dissipation. Nevertheless, this complex behaviour is not general. It depends on the level of entanglement of each block and on the viscoelastic contrast between the two chemical species. Finally, the complex modulus undergoes an abrupt change at the ODT, reflecting the first-order nature of this transition [1,2]. This unambiguous change has been used extensively to detect and study the ODT [4,6–17].

For lamellar and cylindrical phase-separated block copolymers, at least two complex general mechanisms have been invoked to explain the low-frequency linear viscoelastic behaviour: a molecular mechanism involving modified "star-shaped" polymer relaxation processes (i.e. mainly arm retraction) [18,19] and a microstructural mechanism involving deformation of oriented structures and defects at intermediate and global length scales [20–25]. However, if the molecular weight is below the entanglement threshold, the "star-shaped" retraction process cannot be considered [19,23]. Several authors have attempted to subdivide the low-frequency response of the microstructural mechanism

* Corresponding author.

0032-3861/00/$ - see front matter
PII: S0032-3861(99)00147-0

Table 1
PS/PDMS block copolymers characterisation (see Ref. [5] for details)

Samples	M_n of S blocks[a] (g mol^{-1})	M_n (g mol^{-1})	M_w/M_n[a]	ϕ_{PS}[b]	Microstructure[c]	T_{ODT}[d] (°C)	Decomposition temperature[e] (°C)
D51 (PS-b-PDMS)	8100	13 600	1.20	0.56	Lamellae	585	265
D63 (PS-b-PDMS)	8200	11 700	1.15	0.67	PDMS cylinders	257	250
T50 (PS-b-PDMS-b-PS)	8100	27 800	1.09	0.55	Lamellae	611	280

[a] Determined by GPC.
[b] PS volume fraction estimated using the monomer specific volumes Fox empirical equations for PS and PDMS homopolymer at 100°C.
[c] Determined by TEM from neutral solvent cast films.
[d] ODT temperature as estimated from BLHF theory.
[e] Beginning of thermal decomposition (determined by thermogravimetry analysis).

into two different dynamical regimes [5,10,11,13–17,22–25]. Above an "upper" critical frequency ω_c (which was first introduced by Widmaier et al. [10]), the copolymers appear rheologically simple (according to the time–temperature superposition principle) with molecular modes involving reptation (or arm retraction) and Rouse relaxation processes [26]. Below this critical frequency, the rheological response is mainly dominated by the microstructure and this gives some rheological complexity, especially near the ODT. Studying shear-oriented lamellar diblock copolymers, several authors [22,24,25] have more recently introduced a "lower" critical frequency, termed ω_d. Below ω_d, the rheological response is expected to be dominated mainly by defects and hydrodynamic effects linked to the oriented lamellar texture. As a result of vorticity, the viscoelastic response is expected to be governed by microdomain (i.e. interfacial) deformations at intermediate frequencies, $\omega_d < \omega < \omega_c$.

The objective of this work was to study the rheological behaviour of poly(styrene–dimethylsiloxane) (PS/PDMS) block copolymers and to investigate the influence of the microstructure (lamellar or cylindrical) and the molecular architecture (di- or triblocks) on the rheological response. PS/PDMS has been extensively studied in the past (synthesis, type of microphase and thermal properties [see reference in 5], but to our knowledge there is no published rheological study of this particular block copolymer. In the present work, the rheological behaviour of PS/PDMS block copolymers has been investigated by measuring the frequency-dependent storage and loss modulus at the extreme of the linear viscoelastic regime.

2. Experimental

2.1. Samples

Low molecular weight di- (PS-b-PDMS) and triblock (PS–PDMS–PS) copolymers were synthesised by living sequential anionic polymerisation of styrene and hexamethylcyclotrisiloxane. Details of the copolymer synthesis and characterisation have been reported elsewhere [5]. Samples are designated "D" or "T" for di- or triblock respectively followed by the molar percentage of styrene. Three such copolymers were studied. Two are diblock, D51 (51 mol% of styrene) and D63 (63 mol% of styrene), one is a triblock, T50 (50 mol% of styrene). D51 and T50 have a similar styrene content. Note that the length of the central dimethylsiloxane block of T50 is twice that of D51, in order to keep the styrene mole fraction constant. Details of the three samples are given in Table 1.

Transmission electron microscopy (TEM) showed that samples are phase-separated into lamellar (D51 and T50) and cylindrical (D63) microstructures. Differential scanning calorimetry (DSC) measurements showed that these phase-separated samples are strongly segregated, without a significant mixed interphase, at least up to the glass transition temperature of PS domains, near 92°C [5]. Their UCST type ODTs are experimentally unreachable in a reversible way, as thermal decomposition occurs first (see Table 1). The ODT temperatures T_{ODT} were estimated using the BLFH (Brazovskii, Leibler, Fredrickson and Helfand) expression for the critical quench parameter $(\chi N)_{ODT}$ [1,2,14], including the fluctuation corrections

$$(\chi N)_{ODT} \cong 10.7 + 43.2/N^{1/3} \quad \text{for } \phi_{PS} = 0.55 \text{ and } 0.56, \tag{1}$$

$$(\chi N)_{ODT} \cong 12.6 + 63.4/N^{1/3} \quad \text{for } \phi_{PS} = 0.65 \tag{2}$$

where N is the overall diblock (or half the overall triblock) degree of polymerisation and $\chi \approx 106/T$ is the PS/PDMS Flory interaction parameter. In this calculation, the segment length asymmetry and polydispersity corrections are not considered [14,15]. As a result of the pronounced incompatibility between the PS and the PDMS, no one has ever succeeded in experimentally reaching the ODT. Consequently, no precise estimate of χ can be made (by small angle neutron or X-ray scattering or rheological experiments). $\chi \approx 106/T$ is only a rough estimate from PS and PDMS [27] homopolymers' solubility parameters [5]. Calculated T_{ODT} are approximate values given to show

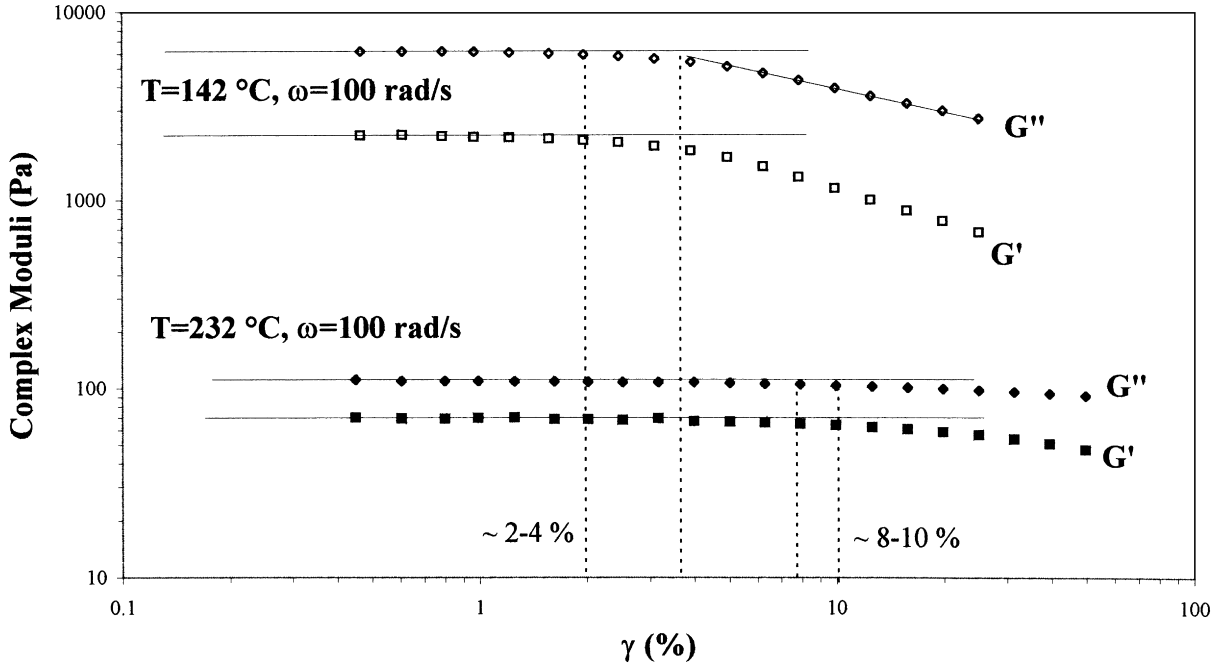

Fig. 1. Loss (G'') and storage (G') moduli versus shear strain amplitude (γ) for the PS/PDMS D63 diblock copolymer, at two different temperatures. ω is the angular frequency.

that the rheological experiments were all performed well below the ODT.

Solvent-cast samples (from neutral solvent [5]) are macroscopically disordered, exhibiting a complex "granular" morphology as seen on a large length scale by depolarised optical microscopy [28]. We have established by depolarised small angle light scattering experiments that a coherent order exists only in small "optical volumes" of typical size 0.8–1 μm [28].

2.2. Rheology

The copolymers were pressure moulded at 250 bar at a temperature of 150°C into discs of 50 mm diameter and 1.5 mm thickness. Before each experiment, the discs were annealed at 110°C under vacuum for more than 24 h. A Rheometrics RMS 800 rheometer was used with parallel-plate geometry (0.8–1.4 mm gap) for dynamical measurements, in the angular frequency range $0.01 \leq \omega \leq 100$ rad s^{-1}. The samples were tested isothermally, with a thermally regulated nitrogen gas purge, at various temperatures between 130 and 230°C (±1°C). This range corresponds to approximately 40°C above the samples' PS microphase glass transition, up to 20–30°C below the beginning of thermal decomposition (see Table 1). For each sample, strain amplitude γ sweep tests at $\omega = 100$ rad s^{-1} were performed at selected temperatures, in order to determine the accessible linear viscoelastic regime (see Fig. 1). The strain amplitude transition from the linear to the non-linear regimes was progressive for all the samples, hence the limit of linearity is expressed by a small range of strain amplitudes denoted as the linear/non-linear region.

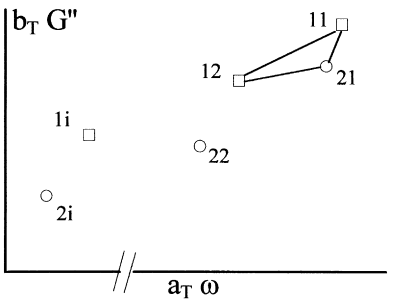

Fig. 2. Schematic illustration of the numerical shift procedure used for calculating master curves.

To restrict the experiments close to the end of the linear regime, frequency dependent G' and G'' measurements were performed between $\gamma = 1\%$ (at 130°C) and $\gamma = 14\%$ (at 230°C). In order to provide sufficient torque, T50 and D51 were studied in the linear regime up to 140°C, with the linear/non-linear transition regime at 150°C and just into the non-linear regime from 160 to 210°C. D63 was studied in the linear regime up to 170°C, and in the non-linear regime from 180 to 230°C.

2.3. High-frequency time–temperature superposition procedure

From the WLF time–temperature superposition principle [29], master curves were constructed shifting the high-frequency part of the modulus curves to a reference

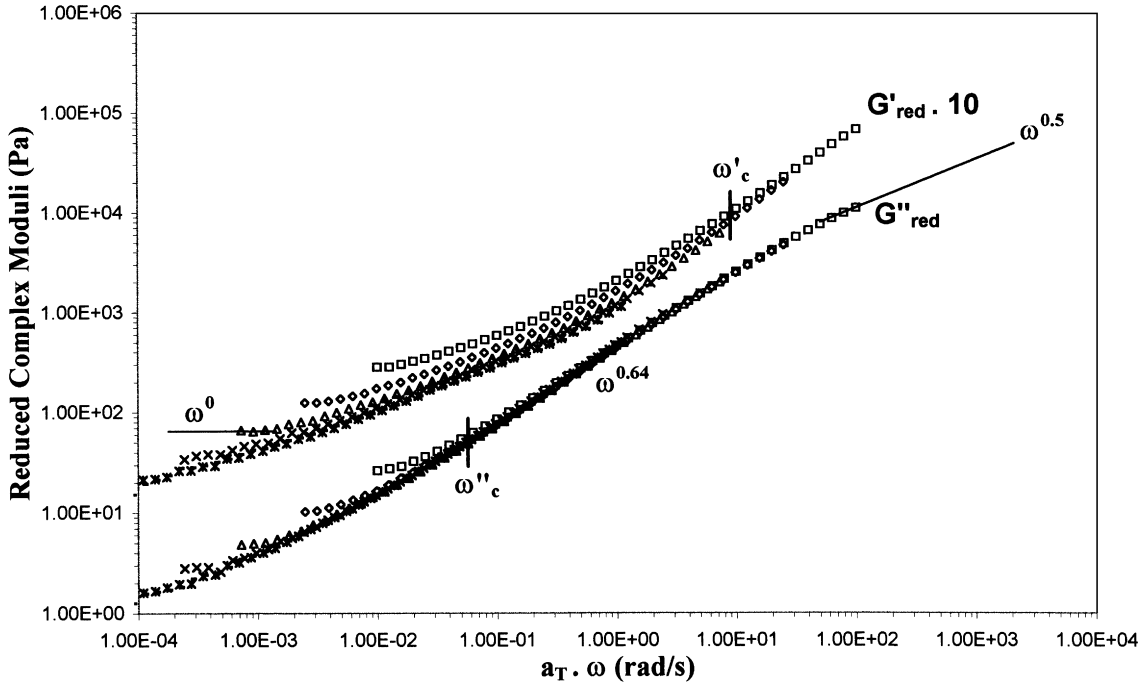

Fig. 3. Reduced dynamical moduli G'_{red} and G''_{red} ($T_0 = 142°C$) for the lamellar triblock T50. G'_{red} has been shifted vertically by one decade for the sake of clarity.

temperature of $T_0 = 142°C$. We have developed a numerical procedure to obtain the horizontal and the vertical shift factors (a_T and b_T respectively), based on the minimisation of the distances between the "high-frequency" points of the shifted curve with those on the reference curve.

The l_i points ($i = 1,2\ldots,21$) are those of the reference curve (see Fig. 2). 21 is the first point of the curve to be shifted, with an intermediate frequency between those of 11 and 12. The distance between 21 and 11 is

$$d_{21}^{1} = \sqrt{(\omega_{21}a_T - \omega_{11})^2 + (G''_{21}b_T - G''_{11})^2}. \quad (3)$$

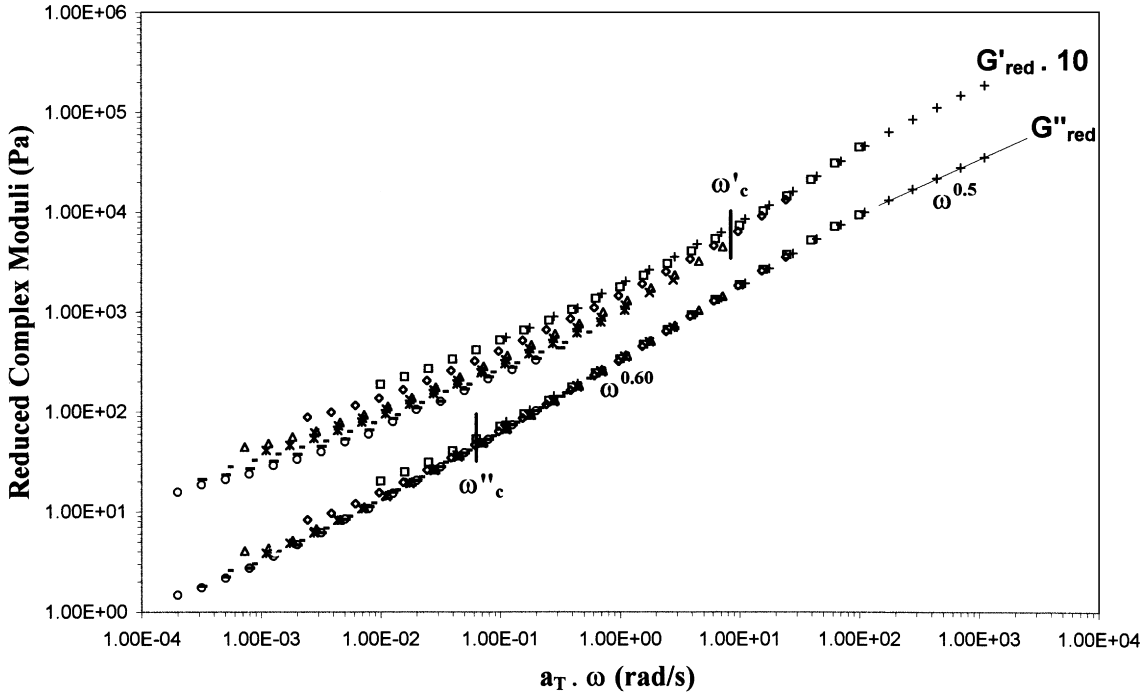

Fig. 4. Reduced dynamical moduli G'_{red} and G''_{red} ($T_0 = 142°C$) for the lamellar diblock D51. G'_{red} has been shifted vertically by one decade for the sake of clarity.

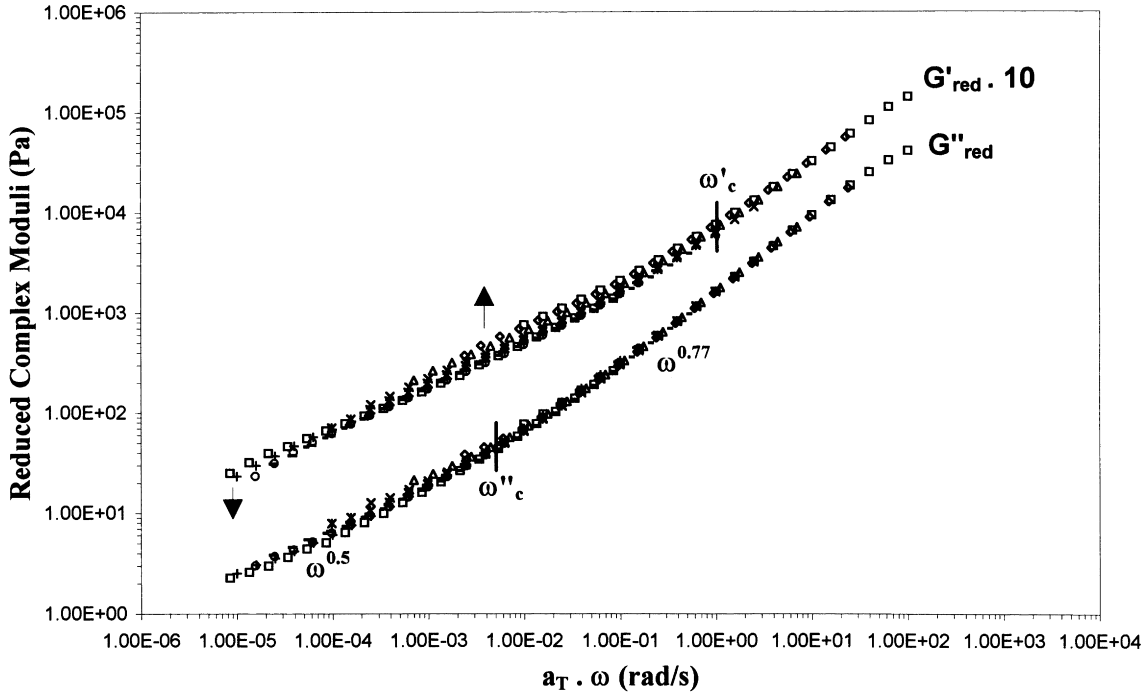

Fig. 5. Reduced dynamical moduli G'_{red} and G''_{red} ($T_0 = 142$°C) for the cylindrical diblock D63. G'_{red} has been shifted vertically by one decade for the sake of clarity.

The distance between 21 and 12 is

$$d_{21}^2 = \sqrt{(\omega_{21}a_T - \omega_{12})^2 + (G''_{21}b_T - G''_{12})^2}. \quad (4)$$

The sum of both distances is a minimum if the 21 point lies on the segment defined by 11 and 12. We define the function $f_n(a_T; b_T)$ as

$$f_n(a_T; b_T) = \sum_{i=1}^{n} d_{2i}^i + d_{2i}^{i+1}, \quad (5)$$

where the sum is performed over the n triplets, which controls the number of points of the high-frequency zone that we want to involved in the shift (n varies from 15 at 130°C to 3 at 230°C). Minimisation of $f_n(a_T; b_T)$ at a fixed n gives the best-fit a_T and b_T values. According to the WLF principle, the specific vertical shift factor $b_T = T_0\rho_0/T\rho$ has to be applied [29], where ρ_0 and ρ are the polymer densities at T_0 and T respectively. The fitted b_T values (without considering the density variations) are systematically close to the simple T_0/T ratio, and the density corrections are neglected. The shift factors that produced superposition of the high-frequency loss modulus data were used to superimpose the storage modulus data (see Section 3).

3. Results

The frequency-dependent viscoelastic properties of the three samples are summarised in Figs. 3–5, as master curves (reduced modulus G'_{red} and G''_{red} versus reduced frequency $a_T\omega$).

3.1. Time–temperature superposition

Despite the PS/PDMS block copolymer intrinsic rheological complexity (at least at the level of the Rouse-segment friction coefficients), the time–temperature superposition principle was applied, shifting the "high-frequency" part of moduli curves to the reference temperature of $T_0 = 142$°C (according to the numerical shift procedure described in the Section 3). The application of the superposition principle was motivated by a general conclusion which has been established by several authors, for different types of lamellar and cylindrical block copolymers [10,11,13–17]. As already described in Section 1, thermorheological complexity in the linear regime is only effective near the ODT, at the low end of the curves below certain critical reduced frequencies, termed ω'_c and ω''_c for the storage and the loss moduli, respectively. Moreover, it has been established that moduli curves superimpose well over several decades of reduced frequency, below the ODT [11,13,20,25], despite the microstructural nature of the samples.

As shown in Figs. 3–5, the shift factors that superimpose the loss modulus curves for PS/PDMS copolymers are inadequate to superimpose those of the storage modulus below a certain reduced frequency ω'_c. There, the low-frequency parts of the G' curves depart from a single master curve. This effect is less pronounced for the cylindrical

Table 2
WLF time–temperature superposition parameters

Samples	c_1[a] (K)	c_2[a] (K)	Deviation temperature between the G'_{red} and G''_{red} a_T shift factors (°C)
D51	6.2	93.1	160
D63	7.1	101.4	180
T50	–	–	150

[a] WLF parameters.

diblock D63. When applying the numerical shift procedure to the storage modulus alone, it is possible to obtain a single master curve for G' (not shown) for the three samples. However, above a certain temperature (see Table 2), a noticeable difference occurs between the a_T values of the loss and the storage modulus. Finally, we note that the low reduced-frequency loss modulus data also fail to superimpose below another reduced frequency ω''_c, which is much lower than ω'_c. This effect is again very small for D63 while it is more pronounced for T50 compared to D51. We thus defined two critical reduced frequencies: ω'_c is defined as the reduced frequency below which the shift factor a_T, determined from the loss modulus, is unable to superimpose the storage modulus data and ω''_c is defined as the reduced frequency below which the loss modulus data depart from the loss modulus master curve. The failure of the time–temperature superposition at low reduced-frequencies (thus below ω'_c and ω''_c) is unambiguously caused by shear-induced morphological changes (see Section 4).

For the two diblocks (D51 and D63), there is agreement between the horizontal shift factor a_T and the WLF Eq. (6):

$$\log(a_T) = \frac{-c_1(T - T_0)}{c_2 + (T - T_0)}. \quad (6)$$

Plotting $(T - T_0) \times \log(a_T)$ against $(T - T_0)$, we obtain a straight line (see Fig. 6), with correlation coefficients close to 0.993 ± 0.001. The fitted WLF constants are given in Table 2. On the contrary, using a_T, we were not able to fit over the entire range of temperature the WLF equation for the triblock (T50) and neither does it fit with the Arrhenius equation [29].

3.2. Frequency-dependent viscoelastic behaviour

As expected, the viscoelastic response of the three samples strongly deviates from the homopolymer single-relaxation-time terminal behaviour below ω'_c (for the storage modulus) and ω''_c (for the loss modulus), reflecting their phase-separated character.

For the diblock D51 (see Fig. 4), the high reduced-frequency part of the viscoelastic response, above ω'_c, resembles that of an unentangled homopolymer [26,29]. The superimposed curves do not exhibit any entanglement plateau and G'_{red} tends towards G''_{red}, which has already reached a $\omega^{0.5}$ Rouse power-law dependence. Around ω'_c, the loss modulus is described by a power-law, $G''_{red} \propto \omega^{0.60}$, over about three decades. Over the same reduced-frequency range, each of the G' curves (which fail to superimpose) progressively increases towards a purely elastic terminal behaviour (i.e. $\lim_{\omega \to 0} G' \propto \omega^0$). Finally, below ω''_c, G''_{red}, also fails to superimpose, and $G''_{red} \approx G'_{red} \to \omega^0$. A similar low-frequency behaviour has already been identified for a quenched PS/PI lamellar diblock of low molecular weight [3,4,23]. This has been attributed to the poor extent of alignment at the global length scale.

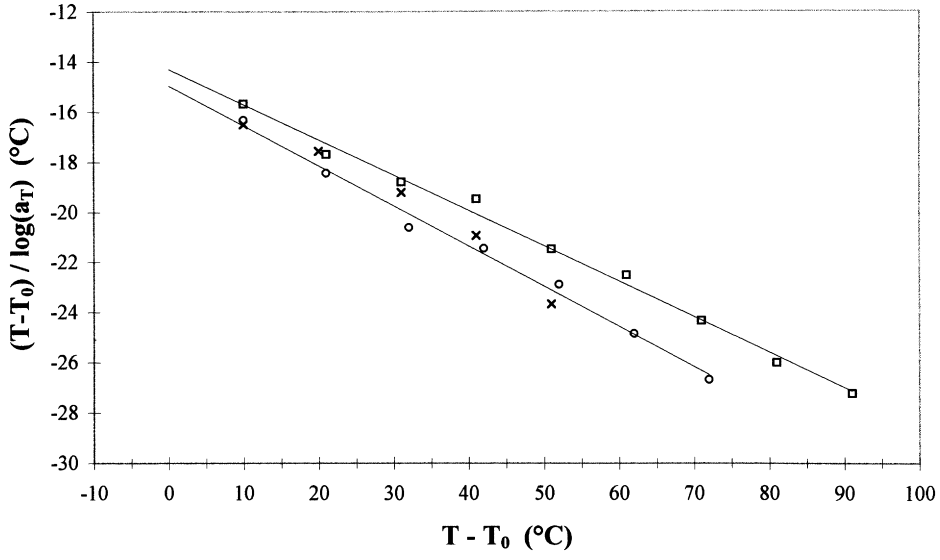

Fig. 6. WLF linear plot of the loss modulus horizontal shift factors for the three copolymers. Open squares correspond to the cylindrical diblock D63, circles to the lamellar diblock D51 and crosses to the lamellar triblock T50.

The viscoelastic response of the triblock T50 is quite similar to that of D51 (see Fig. 3). At high reduced-frequency, above ω_c', the loss and the storage moduli resemble those of an unentangled polymer. Below ω_c', G_{red}'' progressively approaches a $\omega^{0.64}$ power-law dependence over a range of two decades. Over the same reduced frequency range, each of the G' curves (which do not superimpose) progressively reach a final purely elastic dependence. Finally, below ω_c'', the loss modulus data also fail to superimpose and $G_{red}' \approx G_{red}'' \propto \omega^0$.

The viscoelastic response of the diblock D63 (see Fig. 5) is quite different from that of D51 and T50. First, it is difficult to define clearly the two reduced frequencies using the same criteria as for the lamellar block copolymers. ω_c' was arbitrarily chosen as the *x*-coordinate of the first experimental point of the 180°C curve where the numerical shift procedure failed to give the same a_T values. ω_c'' was chosen as the *x*-coordinate of the point which intercepts the terminal and the central power-law dependence (see Fig. 5). Above ω_c', the moduli resemble those produced by an unentangled polymer as for the two other samples. Below ω_c', the loss modulus first shows a $\omega^{0.77}$ power-law dependence over three decades and then follows a $\omega^{0.5}$ power-law dependence below ω_c''. The storage modulus shows a small increase near ω_c''.

4. Discussion

PS/PDMS rheological results show that the material has all the classical characteristics of structured fluids, including microphase-separated lamellar and cylindrical poly(styrene–diene) [7–10,12,23–25], poly(styrene–methylmetacrylate) [30] and poly(olefin–olefin) [10,12–16] di- and triblock copolymers. Nevertheless, some peculiar features need to be discussed. In particular, the low-frequency range shows a departure from the time–temperature superposition principle which can be ranked according to the connectivity of the structure. Finally, a new criterion can be proposed for determining the critical frequencies when the material cannot be heated through the ODT.

4.1. High-frequency rheology ($\omega > \omega_c'$)

For the three samples, we have determined the high reduced-frequency part of the viscoelastic response, introducing a first critical reduced frequency ω_c', in a different manner to Widmaier, Meyer and Bates [10,11]. As the ODT cannot be reached, ω_c' has been defined as the lower limit where the loss and storage moduli superimpose with the same shift factors. Therefore, by definition, samples appear thermo-rheologically simple above ω_c'. We have unambiguously identified a "Rouse-like" viscoelastic behaviour which resembles those of unentangled homopolymers (or disordered block copolymers), which in fact reflects the melted character of the microdomains. Thus, no influence of the microstructure is expected and there is no significant difference between the di- and triblock viscoelastic responses. Considering the low molecular weight of each sample, it is not surprising that copolymer chain dynamics are unaffected by topological constraints (the critical molecular weights for entanglement coupling are near 33 000 g/mol for the PS and near 25 000 g/mol for the PDMS [29]). As a result of the high level of incompatibility between the PS and PDMS chemical species (see Ref. [5] for a general discussion), internal single-block modes of relaxation are excited with probably poor dynamical coupling through the chemical joints.

4.2. Superposition principle

Considering the important difference between the glass transition temperatures of the two blocks (near −123°C and near 92°C for the PDMS and the PS microdomains, respectively, [5]) one may expect the high reduced-frequency parts of the viscoelastic response to be dominated by the PDMS Rouse block modes of relaxation. However, a_T for the two diblock follows a WLF-like temperature dependence. This strongly suggests that the viscoelastic behaviour is controlled by PS blocks. We may imagine that on this time/temperature scale, PDMS blocks of very low molecular weight ($\leq$5500) relax immediately. Over the entire range of temperature, the a_T factor which shifts the loss modulus does not seem to be sensitive to the type of morphology but does seem to be sensitive to the molecular architecture. The cylindrical and lamellar microstructured diblocks exhibit roughly the same a_T dependence (see Fig. 6 and Table 2). On the contrary, the smaller the PDMS block length, the better is the agreement with the WLF equation. For the triblock T50, where the PDMS block is central with twice the molecular weight of D51 (with nearly the same volume fraction and the same morphology), a_T fits neither the WLF equation nor an Arrhenius type relation. This discrepancy, which occurs at high temperature, is due to the double anchoring of the PDMS central block. The fact that the same a_T value can be applied for the loss modulus well below ω_c', where the microstructure plays a role, may be due to the way in which a_T is calculated, considering only a few points in the high-frequency part of the loss modulus curve, and to the fact that the first manifestation of the microdomain deformation is through an elastic response.

4.3. Low-frequency rheology ($\omega < \omega_c'$)

Below ω_c', the a_T shift factors which superimpose the G'' curves of T50, D51 and D63 are not the same as those required for the superposition of the G' curves. As our samples were either near, inside or slightly above the transition from linearity to non-linearity in terms of strain amplitude (see Section 2), this lack of superposition can be attributed to shear-strain-induced morphological changes. In general, if the melt is isotropic (disordered) or, if one of the two phases completely dominates the response over the experimental time scale, the relaxation processes

associated with the loss and the storage mechanisms have the same temperature dependence [12]. Figs.3–5 show that the departure from the master curves increases from the cylindrical D63 diblock, to the lamellar D51 diblock, to the lamellar T50 triblock.

D63, which has the highest PS volume fraction, exhibits a microstructure composed of PDMS cylinders in a PS matrix [5]. This sample is the least sensitive in terms of shear strain amplitude and also provides the best agreement when fitting the WLF equation. As the same shift factors are adequate to roughly superimpose the loss and storage modulus curves, we conclude that despite an existing phase-separated morphology, this sample can accommodate deformation without strong irreversible shear-induced morphological change. Thus, the viscoelastic response is mainly controlled by relaxation processes of the PS matrix. A slight bump is discernible for the storage modulus and at the same time the loss modulus progressively increases. Indeed, at very low reduced-frequency (i.e. high temperature), G'_{red} seems to go slightly downward, which is the opposite behaviour as compared with D51. Such a tendency has also been identified for a macroscopically disordered cylindrical polyolefines diblock copolymer [15] and may be general to "nematic-like" fluids. Bates and co-workers have noticed, when studying macroscopically disordered PEE/PEP diblock, that the bump in G' is linked to the occurrence of composition fluctuations announcing the proximity of the ODT. Considering the theoretical T_{ODT} estimate of 257°C, D63 at 230°C may approach the ODT. This is consistent with the fact that for similar diblock molecular weight the ODT temperature is lower for asymmetric as compared with symmetric samples. However, the D63 ODT could not be reached reversibly due to the occurrence of thermal decomposition at 250°C (see Table 1).

The two lamellar copolymers D51 and T50 show a strong failure of the superposition principle which indicates a significant shear influence on the morphology. The fact that the T50 shift factor does not fit either the WLF or the Arrhenius equations indicates that both PS and PDMS lamellar phases govern the stress relaxation. For D51, the lack of superposition indicates that the stress relaxation cannot be exclusively controlled by the PS lamellae. On the contrary the agreement with the WLF equation indicates a preferential influence of PS microdomains. Thus we conclude that only a small proportion of the PDMS microdomains influence the relaxation on the time/temperature scale considered.

As already mentioned by Larson and co-workers [23], for the case of unentangled nearly symmetric diblock copolymers, the layered structure can resist deformations even at frequencies low enough such that molecular conformations are completely relaxed. This tendency is a characteristic feature of small molecule layered fluids such as smectic liquid crystals and surfactants. Considering these results, we can propose that the departure from the time–temperature master curve, due to the influence of the deformation of the microdomains, is controlled by the connectivity of the microdomain structure. If this microstructure can easily accommodate deformation, its influence on the overall viscoelastic response is not important. Two parameters may control this deformability. One is intrinsic and depends on whether the copolymer has two or three blocks (i.e. one or two anchoring points). As clearly seen in Figs. 3 and 4, the triblock copolymer has strong anchored microdomains that give a large viscoelastic response at the microstructure level, as compared with the diblock. In the latter case, the layers can slip more easily past one another. The second parameter is the type of morphology. Comparing Figs. 4 and 5 shows that lamellar structure gives a stronger departure, at higher frequency, than the cylindrical structure. This is due to the difficulties of deformation of high connectivity structures that cannot easily accommodate deformation without important distortions.

We thus propose that the severity of the departure from the time–temperature superposition principle (i.e. the influence of the viscoelasticity of the microdomain morphology) is a function of the connectivity of the microstructure, increasing from globules to cylinders to layers, and of the molecular architecture, progressing from di- to triblocks.

4.4. Criteria for the influence of the microdomain deformation

The two critical reduced-frequencies ω'_c and ω''_c, have been introduced by Bates et al. [11,13]. They correspond to the values of $a_T\omega$, below which the effect of order and disorder are manifested on either side of the ODT. In other words, ω'_c and ω''_c are the frequency below which the viscoelastic response deviates from the one-relaxation-time terminal behaviour (i.e. $G' \sim \omega^2$ and $G'' \sim \omega$). This deviation is thus supposed to reflect the influence of microdomains on shear stress relaxation processes. There is a problem in defining the location of these critical frequencies when the samples cannot be brought above the ODT. We show here that this problem can be overcome by testing the materials close to their linear/non-linear region. In this region, the material is very sensitive to flow-induced morphological changes, which thus may serve as a bench mark for deducing ω'_c.

5. Conclusion

The viscoelastic properties of three microphase-separated PS/PDMS di- and triblock copolymers have been studied near the end of the linear regime in terms of strain amplitude. The departure below ω'_c and ω''_c from the time–temperature G'_{red} and G''_{red} master curves can be understood considering the connectivity of each of the samples. In particular, lamellar arrangements, through complex granular morphology, are unable to accommodate shear deformation without irreversible distortions i.e. orientation. Several mechanisms were proposed by Kawasaki and Onuki [21]

and by Koppi et al. [22] to take into account microdomain movements that lead to orientation. We cannot at this point consider the validity of these mechanisms without studying the interdependence of the rheology and the morphology of shear-oriented samples.

Acknowledgements

B.V. Loon thanks the EC Erasmus program for a grant. The authors thank the group in Iasi (Prof. B.C. Simionescu and Dr. V. Harabagiu) for providing the samples and C. Peiti for helping to carry out the experiments.

References

[1] Leibler L. Macromolecules 1980;13:1602.
[2] Frederickson GH, Helfand EJ. Chem Phys 1987;87:697.
[3] Winey KI, Patel SS, Larson RG, Watanabe H. Macromolecules 1993;26:2542.
[4] Winey KI, Patel SS, Larson RG, Watanabe H. Macromolecules 1993;26:4373.
[5] Rosati D, Perrin M, Navard P, Harabagiu V, Pinteala M. Macromolecules 1998;31:4301.
[6] Fredrickson GH, Bates FS. Ann Rev Mater Sci 1996;26:501.
[7] Chung CI, Gale JC. J Polym Sci, Polym Phys Ed 1976;14:1149.
[8] Gouinlock EV, Porter RS. Polym Engng Sci 1977;17:535.
[9] Chung CI, Ming LI. J Polym Sci, Polym Phys Ed 1978;16:545.
[10] Widmaier JM, Meyer GC. J Polym Sci, Polym Phys Ed 1980;18:2217.
[11] Bates FS. Macromolecules 1984;17:2607.
[12] Han CD, Kim J. J Polym Sci: Part B 1987;25:1741.
[13] Rosedale JH, Bates FS. Macromolecules 1990;23:2329.
[14] Bates FS, Rosedale JH, Fredrickson GH. J Chem Phys 1990;92:6255.
[15] Almdal K, Bates FS, Mortensen K. J Chem Phys 1992;96:9122.
[16] Gehlsen MD, Almdal K, Bates FS. Macromolecules 1992;25:939.
[17] Rosedale JH, Bates FS, Almdal K, Mortensen K, Wignall GD. Macromolecules 1995;28:1429.
[18] Witten TA, Leibler L, Pincus PA. Macromolecules 1990;23:824.
[19] Rubinstein M, Obukhov SP. Macromolecules 1993;26:1740.
[20] Morrison F, Le Bourvellec G, Winter HH. J Appl Polym Sci 1987;33:1585.
[21] Kawasaki K, Onuki A. Phys Rev A 1990;42:3664.
[22] Koppi KA, Tirrel M, Bates FS, Almdal K, Colby RH. J Phys II (Paris) 1992;2:1941.
[23] Larson RG, Winey KI, Patel SS, Watanabe H, Bruisma R. Rheol Acta 1993;32:245.
[24] Zhang Y, Wiesner U, Spiess HW. Macromolecules 1995;28:778.
[25] Zhang Y, Wiesner U. J Chem Phys 1995;103:4784.
[26] Doi M, Edwards SF. The theory of polymer dynamics. New York: Oxford University Press, 1986.
[27] Chu JH, Rangarajan P, LaMonte Adams J, Register RA. Polymer 1995;36:1569.
[28] Rosati D, Harabagiu V, Navard P. In press.
[29] Ferry JD. Viscoelastic properties of polymers. 3rd ed. New York: Wiley, 1980.
[30] Braun H, Gleinser W, Cantow HJ. J Appl Polym Sci 1993;49:487.